

# RhBMP-2-Loaded PLGA/Titanium Nanotube Delivery System Synergistically Enhances Osseointegration

Yilin Zhang, Lihua Hu, Meng Lin, Shujie Cao, Yiting Feng, and Shengjun Sun\*

Cite This: *ACS Omega* 2021, 6, 16364–16372

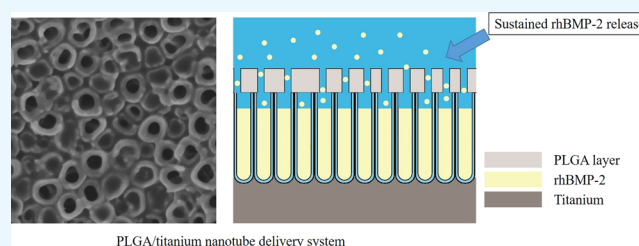
Read Online

ACCESS |

Metrics &amp; More

Article Recommendations

**ABSTRACT:** Although Ti-based implants have been widely used, osseointegration failure can also be found between implants and the surrounding bone tissue, especially in aged patients or in patients with certain systemic diseases. Therefore, in this research, we establish a sustained rhBMP-2 delivery system on a titanium implant surface, an anodic oxidation TiO<sub>2</sub> nanotube layer combined with the PLGA film, to enhance osseointegration. This designed system was characterized as follows: surface topography characterization by SEM and AFM; rhBMP-2 release; and the ability to influence MC3T3 cell adhesion, proliferation, and osteogenic differentiation *in vitro*. Additionally, we evaluated the ability of this system to generate new bone around implants in rabbit tibias by the histological assay and removal torque test. SEM and AFM showed that PLGA membranes were formed on the surfaces of TiO<sub>2</sub> nanotube arrays using 1, 3, and 10% PLGA solutions. The 3% PLGA group showed a perfect sustained release of rhBMP-2, lasting for 28 days. Meanwhile, the 3% PLGA group showed improved cell proliferation and osteogenic mRNA expression levels. In the *in vivo* experiments, the 3% PLGA group had the ability to promote osteogenesis in experimental animals. The anodized TiO<sub>2</sub> nanotube coated with a certain thickness of the PLGA layer was an ideal and suitable rhBMP-2 carrier. This modified surface enhances osseointegration and could be useful in clinical dental implant treatment.



## INTRODUCTION

Recent studies have shown that TiO<sub>2</sub> nanotube (TiNT) arrays on titanium implant surfaces show great application potential in the field of implant materials because of their beneficial osteogenic effect and their high degree of controllability and orderliness.<sup>1,2</sup> Studies have demonstrated that the TiNT layer has the ability to promote bone marrow stromal cell osteogenesis and osteogenic osteoblast function.<sup>1,3</sup> Moreover, the TiNT layer is also suitable for combined use with some cytokines, which play an important role in bone regeneration.<sup>2,4</sup> Until now, BMP-2 has been the most potent growth factor that can promote bone differentiation of stem cells, and it can induce osteogenesis either *in vitro* or *in vivo*.<sup>5</sup> The United States Food and Drug Administration (FDA) has officially approved rhBMP-2 as a clinical therapeutic application, but its application still has some limitations. Although rhBMP-2 has advantageous biosafety properties, it still shows obvious cytotoxicity when used in excess, evident in outcomes including soft tissue edema, ectopic osteogenesis, inflammatory reaction, and even bone resorption.<sup>6</sup> Therefore, choosing a suitable vector that can sustainably release rhBMP-2 is the key to extending its application.

Poly(lactic-co-glycolic acid) (PLGA) is a functional biodegradable polymer organic compound with good biodegradability.<sup>7</sup> *In vivo*, PLGA can be completely decomposed into lactic acid and glycolic acid, which are common substances in

metabolism. Compared with other carrier biomaterials, PLGA has more advantages, including an extended release time and low toxicity.<sup>7,8</sup> The release capacity of PLGA can be controlled within a certain range.<sup>9</sup> It has also been approved by the FDA for clinical use. Current research shows that PLGA can be used as an ideal carrier material for drug delivery systems for the construction of nano/microvectors as sustained-release carriers.<sup>7,10</sup>

We use the anodic oxidation method to prepare TiNT arrays and PLGA coatings on the surface of titanium implants as a sustained release system for the bone growth factor rhBMP-2.<sup>11</sup> Then, we explored the material properties and sustained release effect of the system and studied the *in vitro* effects on the behavior of osteoblasts. Finally, pure titanium implants modified with this system were implanted into experimental animals to evaluate the effect of the system on promoting osseointegration *in vivo*. This study can provide an experimental basis for the development of a new type of

Received: February 18, 2021

Accepted: May 31, 2021

Published: June 15, 2021



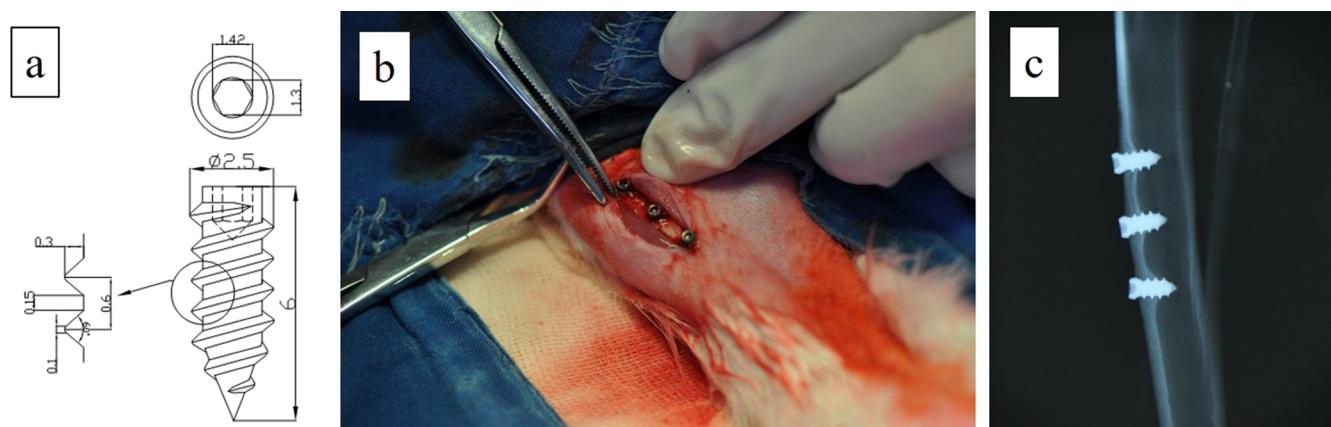


**Figure 1.** Surface characterization by SEM and AFM images of each group. SEM images [a(1)–d(1)]. AFM images [a(2)–d(2)]. Pure chloroform solution-treated {Ctrl group [a(1,2)]}, 1% PLGA solution-treated {1% group [b(1,2)]}, 3% PLGA solution-treated {3% group [c(1,2)]}, and 10% PLGA solution-treated TiNT surface [{10% group [d(1,2)]}. (e) Comparison of nanometer-scale surface roughness values between the control and experimental groups ( $n = 5$  and  $*P < 0.05$ ).

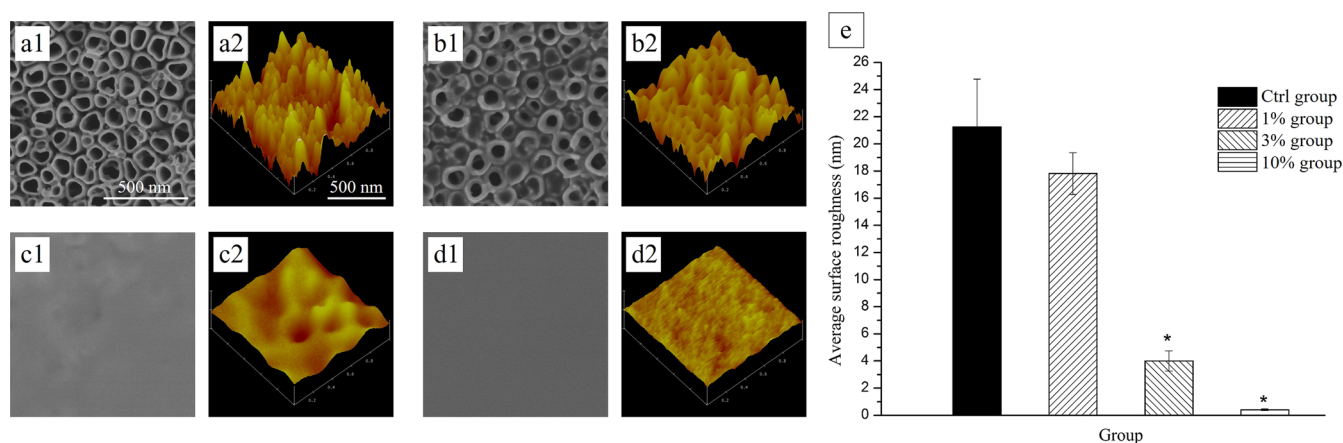


**Figure 2.** *In vitro* rhBMP-2 release kinetics. Cumulative release of rhBMP-2 from the PLGA/TiNT delivery system over the course of 28 days ( $n = 3$ , data represent the mean  $\pm$  s.d.).

dental implant system with good biocompatibility and osseointegration.

## RESULT

**Surface Morphology by SEM.** After anodization, the SEM images showed a regularly aligned array of TiNT with an average diameter of approximately 100 nm on the titanium foil surface [Figure 1a(1)]. With the PLGA solution treatment, layers formed on the surfaces of the samples. The 1% group still showed tube orifice structures, and rhBMP-2 was observed around the TiNT wells [Figure 1b(1)]. The 10% group without any obvious rises and falls or pores [Figure 1c(1),d(1)] indicated a thicker PLGA layer on the surface of TiNT. The three-dimensional AFM images also showed that the concentration of PLGA could influence the samples' morphology. A visible tube orifice structure could still be found in the 3% group [Figure 1c(2)]. In addition, the nanometer-scale surface roughness decreased from the Ctrl group to the 10% group [Figure 1a(2),b(2),c(2),d(2)]. However, only the surface roughness of the 3% group and 10% group showed a significant difference when compared with the Ctrl group [Figure 1e].

**Drug Release Assay.** To reveal the growth factor release capabilities of the rhBMP-2 PLGA/TiNT delivery system,

long-term rhBMP-2 release was measured *in vitro* under physiological conditions (Figure 2). As the release kinetics show in Figure 2, the Ctrl group exhibited higher burst release on the first day, achieving approximately 85% of the growth factor loaded. In the 1% group, up to 80% of rhBMP-2 was released in 3 days, and there was nearly no release after 7 days. For the 3% group, after the initial fast release from day 0 to day 3, the release rate of rhBMP-2 showed a stable sustained release profile within the last 3 weeks. For the 10% group, there was little drug release during the whole experimental period.

**Cell Morphology Assay.** After 4 h of culture, MC3T3 cell morphology on different surfaces was investigated using SEM. Most cells cultured on the 1 and 3% PLGA layers showed a flattened morphology with filopodia (Figure 3b,c), while most cells cultured on the rhBMP-2/TiNT layers showed an elongated morphology with long filopodia (Figure 3a). However, the cells cultured on 10% PLGA layers remained round with barely any filopodia (Figure 3d). The morphologies of MC3T3 cells cultured on different foils were also observed by high-magnification images (Figure 3e–h).

**Cell Proliferation Assay.** The proliferative capability of MC3T3 cells on different foils was evaluated based on CCK-8 assays (Figure 4). Compared with the control, the optical

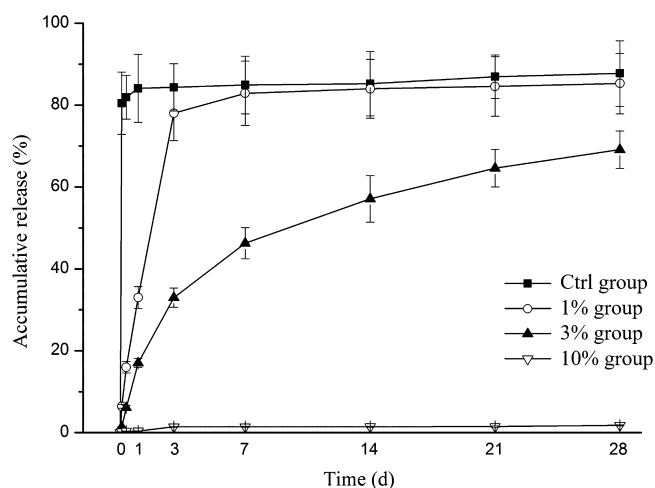


**Figure 3.** Low- and high-magnification SEM images of MC3T3 cells cultured on different surfaces [Ctrl group (a,e); 1% group (b,f); 3% group (c,g); and 10% group (d,h)].

density (OD) values of cells in the 3% group showed a significant increase in cell viability after 1, 3, and 5 days, suggesting that the 3% group enhanced cell proliferation. The OD values of cells in the 10% group were all significantly decreased at each analysis time point, indicating that it inhibited the proliferation of MC3T3 cells.

**Osteogenesis Gene Expression Analysis.** RT-qPCR was used to reveal the gene expression levels of ALP, RUNX2, OPN, and OCN in the MC3T3 cells seeded on the rhBMP-2 PLGA/TiNT layers among four groups (Figure 5). As expected, significant upregulation of ALP expression was observed in cells of the 1% group and 3% group at 7 days, and downregulation of ALP was observed in cells of the 10% group at 7 and 14 days (Figure 5a). As shown in Figure 5b, RUNX2 mRNA expression was significantly increased in the 1% group and 3% group. For further validation of osteogenesis, OPN and OCN expression was quantified. A significant increase was found in OPN and OCN expression in cells cultured on the delivery system of the 1% group and 3% group at 14 days compared to the Ctrl group (Figure 5c,d).

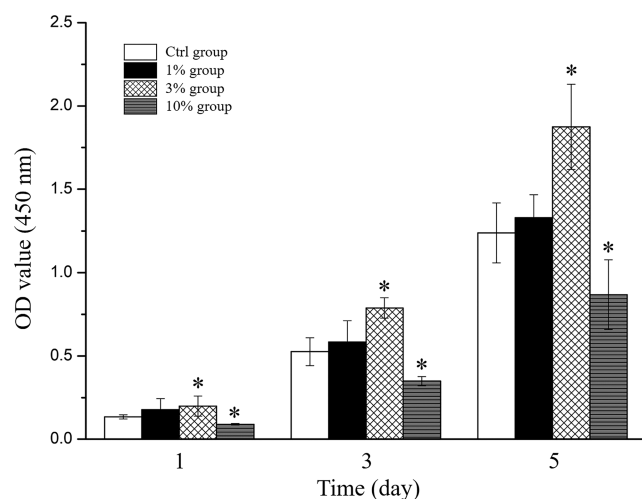


**Figure 5.** Expression levels of the osteogenesis genes (a) ALP, (b) RUNX2, (c) OPN, and (d) OCN in MC3T3 cells seeded on the PLGA/TiNT delivery system for rhBMP-2 (\* $P < 0.05$  and  $n = 3$ , compared with the Ctrl group).

**General Observations.** All rabbits recovered uneventfully following the operation and completed the study as planned through the observation period. No wound infection, implant dislocation, or adverse reactions, such as inflammation or foreign body reaction, were observed in any animal.

**Removal Torque Test.** The results from the removal torque analysis of implants modified with the rhBMP-2 PLGA/TiNT delivery system in the rabbit tibia are described in Table 1. Four weeks after surgery, the highest mean removal torque

**Table 1. Statistical Analyses of the Removal Torque Values for the Groups (Ncm,  $\bar{x} \pm s$ ,  $n = 10$ )**

	Ctrl group	1% group	3% group
4 weeks	$8.5 \pm 2.6$	$9.2 \pm 1.6$	$14.8 \pm 3.2^a$
12 weeks	$13.4 \pm 3.7$	$15.7 \pm 3.8$	$16.7 \pm 2.8$

<sup>a</sup> $P < 0.05$ , compared to the control group.

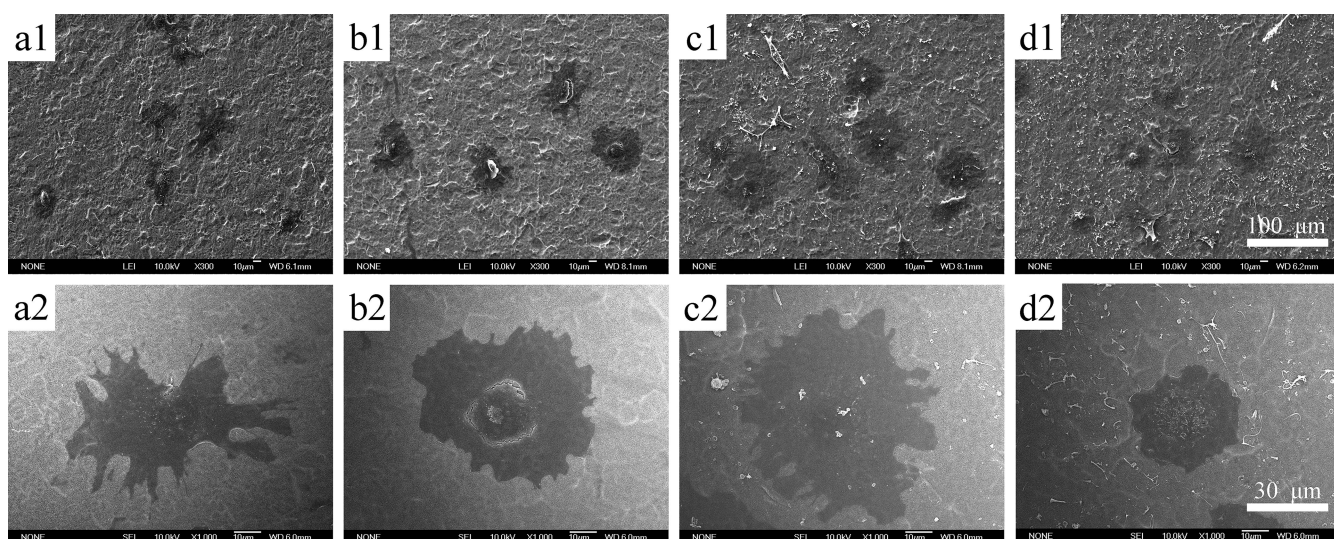


**Figure 4.** Proliferation of MC3T3 cells was estimated by CCK-8 assays (\* $P < 0.05$  and  $n = 3$ , compared with the Ctrl group).

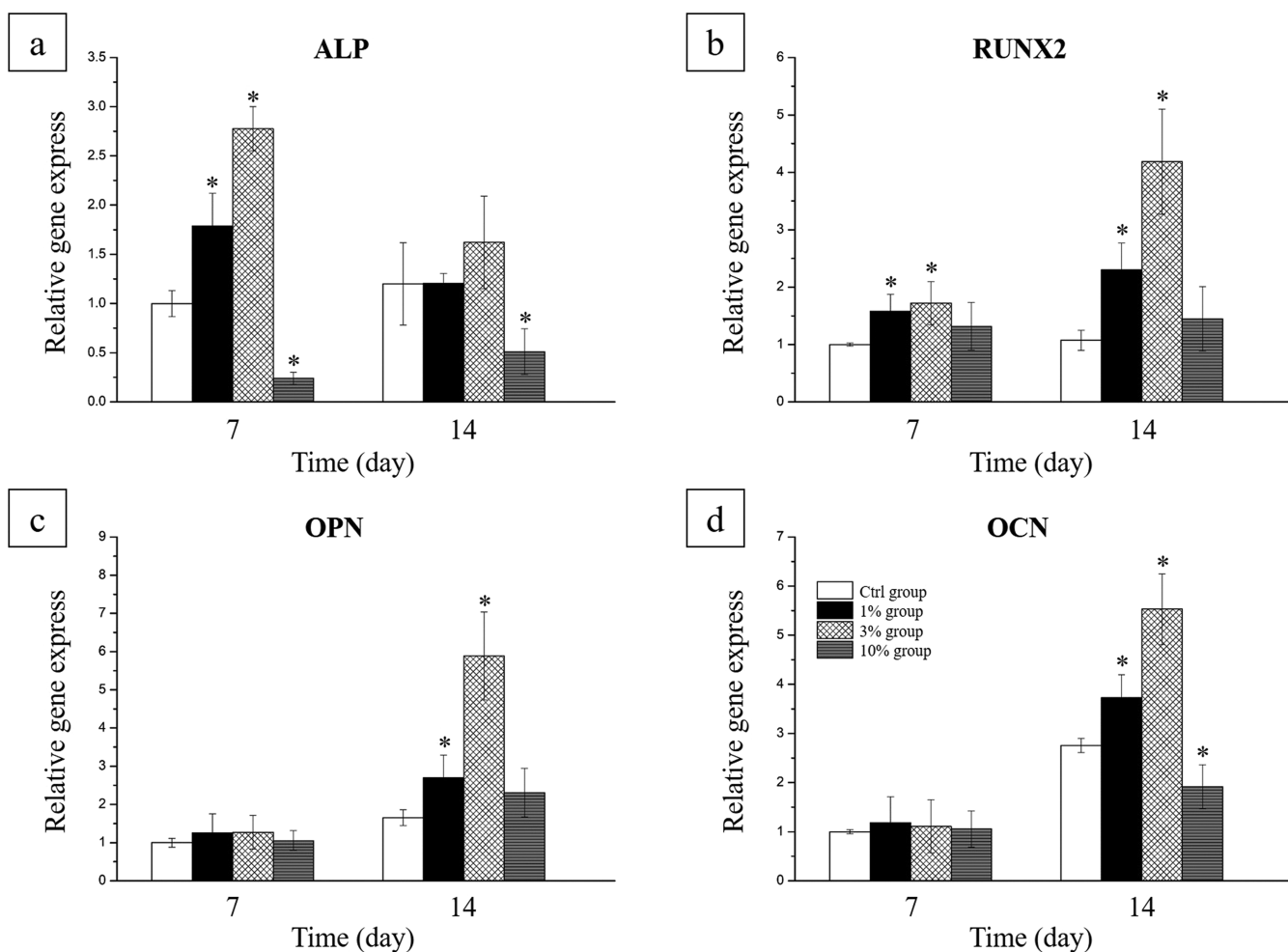


**Figure 6.** Histological evaluation. Histologic sections of implants in rabbit tibia [H&E staining, 4 weeks: [a(1)–c(2)] and 12 weeks: [d(1)–f(2)]. Scale bar: 1.0 mm and 500  $\mu\text{m}$ . The black part indicates the implant screws; the red part indicates bone. (g) Total BIC % ( $n = 6$  and  $*P < 0.05$ , compared with the Ctrl group).

value was found in the 3% group, while the difference between the Ctrl group and 1% group was not statistically significant. At 12 weeks, no significant differences were observed between all three groups.

**Histological Evaluation.** In the fourth week, there was direct contact between the new bone tissues and implants on the surface of implant screws in all groups. In the Ctrl group, there was fibrous tissue between the implant threads and the new bone. In contrast, a well-formed new bone layer with regular bone trabeculae was observed at the interface of implant screws in the 3% group [Figure 6a(1)–c(2)]. Similar results were also found in the BIC measurements (Figure 6g). In the eighth week, bone tissue was more mature than in the fourth week, and a larger mass of new bone could be observed on the surface of implants in the 1% group and 3% group [Figure 6d(1)–f(2)], but the BIC analysis showed no significant difference between groups.

## DISCUSSION

TiNT on titanium implants has attracted great interest in bone tissue engineering. Compared with the relatively smooth surface of pure Ti, TiNT with a diameter in the range of 30–100 nm could enhance cell attachment,<sup>12</sup> preosteoblast differentiation,<sup>13</sup> and osseointegration.<sup>14</sup> Recently, several studies have shown that TiNT is also useful as a drug carrier

material for slow drug release.<sup>15,16</sup> The TiNT layer used here has showed excellent hydrophilicity.<sup>17</sup> Hydrophilic cytokines could be quickly distributed to the whole surface of the sample after adding on the sample. BMP-2 has been proved that it can promote bone differentiation of stem cells and induce osteogenesis either *in vitro* or *in vivo*. However, considering treatment costs and excessive side effects, choosing a suitable vector that can sustainably release rhBMP-2 is required. In our studies, a sustained release delivery system for rhBMP-2 based on PLGA/TiNT was established.

In an aqueous environment, PLGA can be completely decomposed into lactic acid and glycolic acid, which are finally broken down to form energy, water, and carbon dioxide.<sup>18</sup> The PLGA degradation rate is considerably affected by the size and shape of the PLGA. PLGA with a higher ratio of surface area to volume leads to faster degradation.<sup>19,20</sup> Based on our these research studies, 3 and 10% PLGA led to a uniform coating on the TiNT surface, and the 10% PLGA group is obviously thicker than other groups.<sup>11</sup> Ma *et al.* also reported a similar surface morphology.<sup>25</sup> RhBMP-2 release profiles are quite different for this delivery system with different concentrations of PLGA. It is concluded that the thickness of the PLGA film affects the drug release process. The 3% group showed a slow and sustained release pattern at 28 days. Therefore, a highly localized rhBMP-2 concentration

could be maintained during the osseointegration period. These PLGA layers (50% LA and 50% GA) exhibited an approximately 1–2 month degradation rate.<sup>18</sup> Little rhBMP-2 was detected in the 10% group during this period because of the thickness of the PLGA.

After 4 h of culture, most cells cultured on the rhBMP-2/TiNT layers showed an elongated morphology with long filopodia. This cell morphology might be due to the combined actions of TiNT and rhBMP-2, which generate synergistic effects on optimized early adhesion.<sup>17,21</sup> The smooth PLGA surface has negative influence on cell adhesion, because of its hydrophobic property,<sup>22,23</sup> while rough PLGA surfaces could guide and encourage the migration of osteoblasts.<sup>24</sup> In our study, the cells cultured on 10% PLGA layers were round with barely any filopodia. Improved cell adhesion and elongated morphologies were observed with 1 and 3% PLGA. These phenomena may be explained by the morphologies of the PLGA/TiNT substrates and release of rhBMP-2. The 1 and 3% groups show a combined morphology of tube orifice and membrane structures. Wang *et al.* have reported that cell adhesion on PLGA/TiNT improved significantly because the synergistic effect of TiNT and PLGA offered more bioactive receptor binding sites for the attachment of filopodia of cells.<sup>23</sup> When 10% PLGA was applied to TiNT, the tube orifice structure disappeared, and a smooth low roughness surface was exhibited, which affected cell adhesion. Ma *et al.* have indicated that the wettability of the PLGA/TiNT layer also affected osteoblast cell adhesion.<sup>25</sup> The 3% PLGA evidently promoted MC3T3 cell proliferation at 1, 3, and 5 days on the condition of same TiNT and equal amounts of rhBMP-2. Studies reported that rhBMP-2, TiNT, and nanostructured PLGA each promoted the osteoblast cell proliferation.<sup>17,26–28</sup> The loading of rhBMP-2 on the titania surfaces, such as TiNT, also shows a positive action on cell proliferation.<sup>27,29</sup> We assumed that the PLGA/TiNT layer with an appropriate amount of rhBMP-2 displayed higher cell proliferation ability. The exact mechanism deserves further investigation. The cell proliferation of the 10% group was lower than the other groups. This result is attributed to the low roughness PLGA layer which has negative influence on the proliferation of cells on the samples.<sup>23</sup>

The final goal of the rhBMP-2 release is bone regeneration, so we explored the osteogenesis ability of the rhBMP-2-loaded PLGA/titanium nanotube delivery system through measuring the gene expression levels of osteogenic markers. As shown in experiment results, the 1 and 3% groups displayed higher ALP expression at 7 days, which was in accordance with our former study.<sup>11</sup> Moreover, these two groups displayed higher Runx2 expression at 7 and 14 days and higher OPN expression and higher OCN expression at 14 days. This phenomenon was closely related with the release profile of rhBMP-2, for that the 3% group has released an appropriate amount of rhBMP-2. For the Ctrl and 1% group, the dose of rhBMP-2 released was too high at the first week, so the osteogenic differentiation of MC3T3 cells was inhibited.<sup>30</sup> When it comes to the second week, the Ctrl and 1% group have not released enough rhBMP-2, compared to the 3% group. For the 10% group, there was little rhBMP-2 secreted during the whole experimental process. What is more, compared with the Ctrl group, Figure 1 shows that the 10% group lacked proper surface roughness,<sup>31</sup> so its osteogenesis ability was even lower than the Ctrl group. Zhang *et al.* also found that the osteogenesis of BMSCs cultured with TiO<sub>2</sub>-Lyo-Tre-BMP-2 was statistically higher than that of BMSCs cultured with TiO<sub>2</sub>-

BMP-2.<sup>32</sup> These results implied that a delivery system that slowly released the rhBMP-2 dose improved cell differentiation.<sup>32,33</sup>

Qualitatively and quantitatively, the results from the *in vivo* study, carried out by implanting the modified implant screws in rabbit tibia implant models, confirm that the rhBMP-2-loaded PLGA/titanium nanotube delivery system enhance bone regeneration. On H&E staining slices, significantly higher bone regeneration was observed in the 3% group when compared to the Ctrl group. The BIC % of the 3% group was also significantly higher than the Ctrl group at the fourth week, in accordance with the removal torque test results. However, the 1% group did not show significant advantage compared to the Ctrl group, and this can be attributed to the burst release of rhBMP-2 at first 3 days of these groups, and there was no appropriate amount of rhBMP-2 released during 4 weeks. These results show the beneficial effort of the PLGA/titanium nanotube as a growth factor carrier, for it protects the growth factor from degradation *in vivo*. There was no difference in bone formation ability among the three groups after 12 weeks of implantation. We conclude that 3% PLGA/rhBMP-2-modified TiNT layers promoted new bone formation on the implant surface and enhanced bonding strength between the new bone and the implant. Research from Yang and others showed that rhBMP-2 has considerable ability not only to stimulate bone formation but also to promote implant osseointegration.<sup>34</sup> In keeping with their studies, we revealed better osseointegration on the surface of the rhBMP-2-loaded PLGA/titanium nanotube delivery system-modified implant screws, especially when it comes with an appropriate PLGA layer, which further confirmed the *in vitro* results.

## CONCLUSIONS

This study showed that anodic oxidation of TiNT with a certain PLGA layer thickness was an ideal and suitable rhBMP-2 carrier. This modified rhBMP-2 PLGA/TiNT surface promoted greater adhesion, proliferation, and osteogenic differentiation of MC3T3 cells *in vitro* and enhanced bone generation *in vivo* compared with the rhBMP-2/TiNT surface. The PLGA/TiNT delivery system for rhBMP-2 in our current study has great potential for use in dental implants. This PLGA/TiNT delivery system might be used as a vector for other cytokines or agents, such as antibacterial agents and anti-inflammatory agents.

## METHODS

**TiNT Preparation.** TiNT was fabricated on the surface of titanium foil (0.25 mm thick, 99.5% purity; Alfa Aesar, Tianjin, China) by anodization.<sup>11</sup> The brief process is as follows: the foil was placed in distilled water, followed by ultrasonic cleaning in anhydrous ethanol and distilled water for 5 min to remove any contamination. Then, samples were put in mixed acid [a solution containing 3% (v/v) 70% HNO<sub>3</sub> and 2% (v/v) 48% HF] for another 5 min to remove the oxidation layer on the titanium surface. The pretreated foil was linked to the anode of the potentiostat, the counter electrode was made using platinum, and the electrolyte was created using 1 M H<sub>3</sub>PO<sub>4</sub> with 0.5 wt % HF at a voltage of 20 V and room temperature (between 15 and 25 °C) for 3 h. Eventually, after calcination at 450 °C for 3 h, samples were cut into 1 × 1 cm<sup>2</sup> pieces.

**Preparation of the PLGA/TiNT Delivery System for rhBMP-2.** The 0.1 mg/mL rhBMP-2 solution (R&D Systems, Minneapolis, MN, USA) was added to the surface of the TiNT plates at a concentration of 10  $\mu\text{L}/\text{cm}^2$ . Then, plates were freeze-dried at  $-46\text{ }^\circ\text{C}$  in a freeze dryer. PLGA (LA/GA ratio of 50/50; Sigma-Aldrich, St. Louis, MO, USA) chloroform solution was prepared at concentrations of 1, 3, and 10% (w/v). Plates were then dipped in these solutions rapidly and kept at  $4\text{ }^\circ\text{C}$  for 5 min.<sup>11,25</sup> Experimental plates were divided into the 1% group (1% PLGA), 3% group (3% PLGA), and 10% group (10% PLGA), and the group designation was recorded. The control plate was immersed into a pure chloroform solution and recorded as the Ctrl group. All specimens were stored at  $-80\text{ }^\circ\text{C}$  under sterile conditions.

**Surface Topography Characterization.** After gold was sprayed using a HUMMER SputterCoater (Anatech Ltd., Springfield, VA, USA), samples were observed by scanning electron microscopy (SEM, FEI SIRION 200, Hillsboro, USA). Atomic force microscopy (AFM, Bioscope II, Digital Instruments, USA) was used to scan the samples in the tapping mode ( $1 \times 1\ \mu\text{m}^2$ , 0.5 Hz). The results were then analyzed using Nano Navi software (ver. 5.00, Japan) to calculate the nanometer-scale surface roughness of the surface.

**Drug Release Assay.** To measure the amount of rhBMP-2 released from PLGA/TiNT surfaces, the specimens were placed in 24-well cell culture plates with 1 mL of PBS for each specimen. After that, the specimens were placed on a constant temperature shaker, rotating at  $36\text{ }^\circ\text{C}$  with 70 rpm. The amount of rhBMP-2 in each well was measured using the rhBMP-2 ELISA kit (R&D Systems, Minneapolis, MN, USA) at the following time points (2 and 8 h; 1, 3, 7, 14, 21, and 28 d).

**Cell Culture.** MC3T3-E1 preosteoblasts (Cell Bank of the Chinese Academy of Sciences, Shanghai, China) were cultured in  $\alpha$ -MEM (alpha-minimum essential medium; Gibco, USA), which was supplemented with 1% antibiotics (streptomycin and penicillin, HyClone, USA) and 10% heat-inactivated fetal bovine serum (HyClone, USA) in a humidified atmosphere of 5%  $\text{CO}_2$  at  $37\text{ }^\circ\text{C}$ . Cells were trypsinized and then seeded onto samples at a density of  $1 \times 10^4$  cells per well in 24-well plates. The osteogenic medium (50  $\mu\text{g}/\text{mL}$  ascorbic acid and 10 mM  $\beta$ -glycerol phosphate) was changed the next day. The cell medium was changed every 3 days.

**Cell Morphology Observation.** After culture for 4 h, plates were rinsed with PBS and fixed with 2.5% glutaraldehyde. After spraying them gold, cells on samples were observed under SEM.

**Cell Proliferation Test.** Cell proliferation was measured using the CCK-8 assay (Beyotime Biotechnology, Jiangsu, China). MC3T3 cells were seeded onto samples for 1, 3, and 5 days. Then, cells were cultured in medium containing 10% CCK-8 for an additional 2 h at  $37\text{ }^\circ\text{C}$ . Finally, the optical density in nanometers was detected at 450 nm using a spectrophotometer (Safire<sup>2</sup> TECAN, Seestrasse, Switzerland).

**Gene Expression Assay.** Quantitative real-time RT-PCR (qRT-PCR) was conducted to detect ALP, RUNX2, OPN, and OCN mRNA expression. After 7 and 14 days of cultivation, total RNA was extracted from cells on different plates using the RNA purification kit (TRIzol Plus, Invitrogen, USA) following the manufacturer's instructions. Complementary DNA was synthesized from the extracted RNA using the Prime-Script\_RT reagent kit (Takara Bio, Shiga, Japan). Specific primers for PCR amplification are shown in Table 2. qRT-PCR

**Table 2. Nucleotide Sequences for Real-Time RT-PCR Primers**

gene	primer sequence (forward/reverse)
ALP	5'-GCAGATTGACCACGGACACTATG-3' 5'-TTCTGCTCATGGACGCCGTGAAGC-3'
RUNX2	5'-CCGCACGACAA CCGCACCAT-3' 5'-CGTCCGGCCC ACAATCTC-3'
OPN	5'-TCACCATTCCGGATGAGTCTG-3' 5'-ACTTGTGGCTCT GATGTTCC-3'
OCN	5'-AGGAGGGCAATAAGGTAGTGAA-3' 5'-TACCATAGATGCGTTTGTAGGC-3'
$\beta$ -action	5'-ATCTCCTTCTGCATCCTGTGCG-3' 5'-TGGACTTCGAGCAAGAGATGG-3'

was performed with the following cycling conditions:  $95\text{ }^\circ\text{C}$  for 180 s followed by 40 cycles of  $95\text{ }^\circ\text{C}$  for 10 s,  $60\text{ }^\circ\text{C}$  for 30 s, and  $72\text{ }^\circ\text{C}$  for 10 s. All reactions were performed in triplicate. The target gene expression was normalized to  $\beta$ -actin, and the relative expression was analyzed with the  $2^{-\Delta\Delta C_t}$  method.

**Implant Preparation.** In this research, a specially made screw-shaped titanium implant (Figure 7a, commercially pure Ti grade 1 pure titanium, Jinfu Titanium industry, Shanghai) was used. The surface area of this titanium implant was estimated to be  $47.9\text{ mm}^2$  by the following formula ( $a$ : inner diameter;  $b$ : outer diameter;  $c$ : pitch; and  $d$ : body length).<sup>35</sup>

$$\text{Surface area} = \pi \times \left\{ \left( \frac{b}{2} \right)^2 - \left( \frac{a}{2} \right)^2 \right\} \times \frac{d}{c} \times 2 \times \frac{2}{\sqrt{3}}$$

These titanium samples were prepared as described previously to fabricate TiNT and to immobilize rhBMP-2. Subsequently, some samples were immersed in the PLGA solution and stored at  $-80\text{ }^\circ\text{C}$  before animal experiments. Based on previous *in vitro* experiments, 1% or 3% (w/v) PLGA chloroform solution was chosen for further study.

**Surgery Procedure.** The animal study design and protocol were approved by the Ethical Committee of the Stomatology School of Shandong University, Jinan, China (no. GD201604). This study included 16 female New Zealand rabbits initially aged approximately 24 weeks and that were skeletally mature, weighing 3.0–4.0 kg. During the experiment, all rabbits received three implants in each tibia: Ctrl, 1, and 3% groups (Figure 7b). Rabbits were randomly divided into the 4 week removal torque group, 12 week removal torque group, 4 week histological evaluation group, and 12 week histological evaluation group.

The rabbits were anesthetized with a marginal ear vein injection of 0.7% sodium pentobarbital solution (6 mL/kg). Before surgery, the skin of the hind limb was shaved and disinfected by applying chlorhexidine and 75% ethanol, and local anesthesia with 2% lidocaine was also performed. Then, a 25 mm incision was created on the medial side of the tibia. Under abundant cold sterile saline irrigation, the implant sites were prepared using a 2.3 mm drill at a speed lower than 800 rpm. There was a 7–9 mm distance between the centers of two adjacent implants. After preparation, three samples were implanted perpendicular to the bone surface in each tibia (Figure 7c). The muscular and subcutaneous planes were sutured plane by plane, and the surgical site was disinfected. Postoperatively, all rabbits received an intramuscular dose of antibiotics (penicillin, 800,000 U) for 3 days.

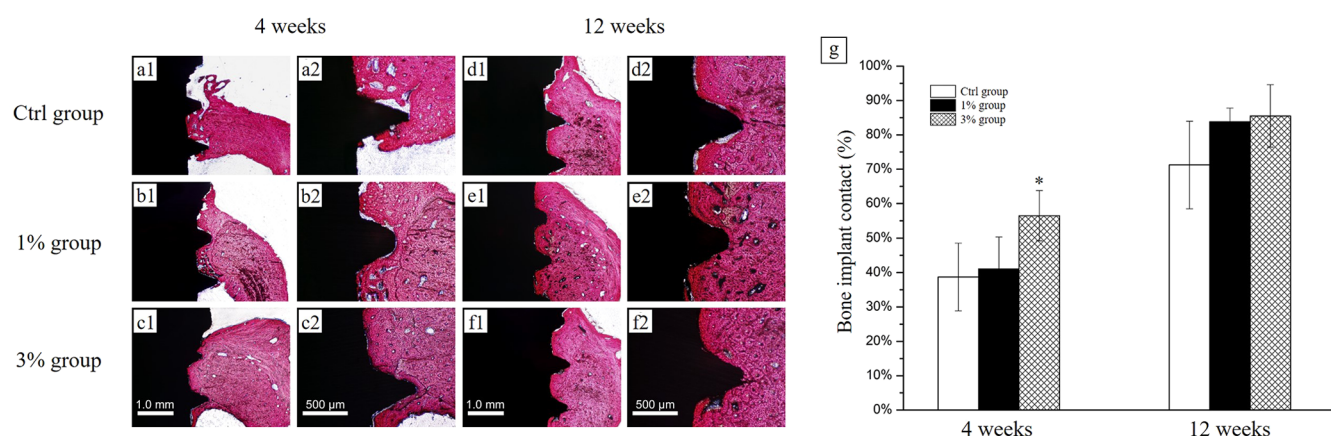


**Figure 7.** (a) Implant screws used in the experiment (units in the figure: mm). (b) Screws implanted in experimental animals. (c) X-ray diagram of the implanting location.

All experimental rabbits were housed in the standard animal experiment center with normative laboratory water and diet. They were observed daily by inspection of mental and dietary conditions and if there was any swelling, infection, or wound dehiscence at the surgical site. At 4 and 12 weeks, the rabbits were euthanized with an overdose of pentobarbital (New Asia pharmaceutical, Shanghai, China; 180 mg/kg body weight).

**Removal Torque Test.** After the sacrifice of five animals in each analysis period (4 and 12 weeks), the tibia bones with implants were removed and processed immediately for the measurement of the MRT (maximum removal torque) with the torque testing machine (CME, Técnica Industrial Oswaldo Filizola, SP, Brazil). The maximal force was measured by removing the samples *via* an anticlockwise rotation, and the mean MRT values were calculated for each group.

**Histological Evaluation.** Three rabbits were sacrificed at postoperative 4 and 12 weeks. The sample portions of tibia bones from sacrificed animals were immersed in 10% buffered formalin. These implant bone blocks were maintained in this solution for 7 days. Then, the blocks were dehydrated in a progressive series of alcohol solutions (60–100%) and embedded in glycol methacrylate (Technovit 7200 VLC, Hereaus Kulzer, Germany). The blocks were sectioned transversely along the longitudinal axis of the implant using IsoMet 1000 (Buehler, Lake Bluff, USA). The samples were polished and ground to a final thickness of 30 μm. The slides were stained with H&E (hematoxylin and eosin), and the regenerated osseous tissue was evaluated. The measurement of BIC % (bone to implant contact percentage) was performed at  $\times 100$  magnification using an optical microscope (E200, Nikon, Tokyo, Japan) and calculated using ImageJ software (ImageJ ver.6, National Institute of Mental Health, MD, USA) by assessing the amount of mineralized bone tissue in direct contact with the implant surface. The BIC % was measured manually by analyzing histomorphometrical images of the entire cortical bone. The ratios of two sides of each sample were determined, and the mean BIC % for each implant was then calculated.

**Statistical Analysis.** We analyzed the data using SPSS version 19.0 software (SPSS Inc., Chicago, IL, USA). Data are presented as the mean value  $\pm$  standard deviation (SD). Statistical analysis was performed using one-way ANOVA to analyze intragroup differences. A threshold of  $P < 0.05$  was considered to indicate a statistically significant difference.

## AUTHOR INFORMATION

### Corresponding Author

**Shengjun Sun** – Department of Prosthodontics, School and Hospital of Stomatology, Cheeloo College of Medicine, Shandong Key Laboratory of Oral Tissue Regeneration & Shandong Engineering Laboratory for Dental Materials and Oral Tissue Regeneration, Shandong University, Jinan, Shandong 250012, China; [orcid.org/0000-0001-6381-9548](https://orcid.org/0000-0001-6381-9548); Phone: +86 531 8838 2972; Email: [sunshengjun@sdu.edu.cn](mailto:sunshengjun@sdu.edu.cn); Fax: +86 531 8838 2923

### Authors

**Yilin Zhang** – Department of Stomatology, Shandong Provincial Hospital Affiliated to Shandong First Medical University, Jinan, Shandong 250021, China; Department of Stomatology, Shandong Provincial Hospital, Cheeloo College of Medicine, Shandong University, Jinan, Shandong 250021, China

**Lihua Hu** – Department of Stomatology, Shandong Provincial Hospital Affiliated to Shandong First Medical University, Jinan, Shandong 250021, China; Department of Stomatology, Shandong Provincial Hospital, Cheeloo College of Medicine, Shandong University, Jinan, Shandong 250021, China

**Meng Lin** – School of Chemistry and Chemical Engineering, Shandong University, Jinan 250012, China; [orcid.org/0000-0002-5910-5654](https://orcid.org/0000-0002-5910-5654)

**Shujie Cao** – School and Hospital of Stomatology, Cheeloo College of Medicine, Shandong Key Laboratory of Oral Tissue Regeneration & Shandong Engineering Laboratory for Dental Materials and Oral Tissue Regeneration, Shandong University, Jinan, Shandong 250012, China

**Yiting Feng** – School and Hospital of Stomatology, Cheeloo College of Medicine, Shandong Key Laboratory of Oral Tissue Regeneration & Shandong Engineering Laboratory for Dental Materials and Oral Tissue Regeneration, Shandong University, Jinan, Shandong 250012, China

Complete contact information is available at:

<https://pubs.acs.org/10.1021/acsoomega.1c00851>

### Funding

This work was supported by the Natural Science Foundation of Shandong Province (ZR2019PH031, ZR201702230238, and ZR2020MH189), Young Scholars Program of Shandong

University (2018WLJH79), and Project of Medical Science and Technology Development of Shandong Province (2018WS269).

## Notes

The authors declare no competing financial interest.

## REFERENCES

- (1) Sarraf, M.; Nasiri-Tabrizi, B.; Yeong, C. H.; Madaah Hosseini, H. R.; Saber-Samandari, S.; Basirun, W. J.; Tsuzuki, T. Mixed oxide nanotubes in nanomedicine: A dead-end or a bridge to the future? *Ceram. Int.* **2021**, *47*, 2917–2948.
- (2) Jafari, S.; Mahyad, B.; Hashemzadeh, H.; Janfaza, S.; Gholikhani, T.; Tayebi, L. Biomedical Applications of TiO<sub>2</sub> Nanostructures: Recent Advances. *Int. J. Nanomed.* **2020**, *15*, 3447–3470.
- (3) Huang, J.; Zhang, X.; Yan, W.; Chen, Z.; Shuai, X.; Wang, A.; Wang, Y. Nanotubular topography enhances the bioactivity of titanium implants. *Nanomedicine* **2017**, *13*, 1913–1923.
- (4) Jia, H.; Kerr, L. L. Sustained ibuprofen release using composite poly(lactic-co-glycolic acid)/titanium dioxide nanotubes from Ti implant surface. *J. Pharm. Sci.* **2013**, *102*, 2341–2348.
- (5) Alhussaini, A. H. A. Effect of Platelet-Rich Fibrin and Bone Morphogenetic Protein on Dental Implant Stability. *J. Craniofac. Surg.* **2019**, *30*, 1492–1496.
- (6) James, A. W.; LaChaud, G.; Shen, J.; Asatrian, G.; Nguyen, V.; Zhang, X.; Ting, K.; Soo, C. A Review of the Clinical Side Effects of Bone Morphogenetic Protein-2. *Tissue Eng., Part B* **2016**, *22*, 284–297.
- (7) Mir, M.; Ahmed, N.; Rehman, A. U. Recent applications of PLGA based nanostructures in drug delivery. *Colloids Surf., B* **2017**, *159*, 217–231.
- (8) Liu, Y.; Castro Bravo, K. M.; Liu, J. Targeted liposomal drug delivery: a nanoscience and biophysical perspective. *Nanoscale Horiz.* **2021**, *6*, 78.
- (9) Kapoor, D. N.; Bhatia, A.; Kaur, R.; Sharma, R.; Kaur, G.; Dhawan, S. PLGA: a unique polymer for drug delivery. *Ther. Deliv.* **2015**, *6*, 41–58.
- (10) Wang, X.; Qi, F.; Xing, H.; Zhang, X.; Lu, C.; Zheng, J.; Ren, X. Uniform-sized insulin-loaded PLGA microspheres for improved early-stage peri-implant bone regeneration. *Drug Deliv.* **2019**, *26*, 1178–1190.
- (11) Sun, S.; Zhang, Y.; Zeng, D.; Zhang, S.; Zhang, F.; Yu, W. PLGA film/Titanium nanotubes as a sustained growth factor releasing system for dental implants. *J. Mater. Sci. Mater. Med.* **2018**, *29*, 141.
- (12) Su, E. P.; Justin, D. F.; Pratt, C. R.; Sarin, V. K.; Nguyen, V. S.; Oh, S.; Jin, S. Effects of titanium nanotubes on the osseointegration, cell differentiation, mineralisation and antibacterial properties of orthopaedic implant surfaces. *Bone Joint J.* **2018**, *100-B*, 9–16.
- (13) Voltrova, B.; Hybasek, V.; Blahnova, V.; Sepitka, J.; Lukasova, V.; Vocetkova, K.; Sovkova, V.; Matejka, R.; Fojt, J.; Joska, L.; Daniel, M.; Filova, E. Different diameters of titanium dioxide nanotubes modulate Saos-2 osteoblast-like cell adhesion and osteogenic differentiation and nanomechanical properties of the surface. *RSC Adv.* **2019**, *9*, 11341–11355.
- (14) Han, C.-M.; Kim, H.-E.; Koh, Y.-H. Creation of hierarchical micro/nano-porous TiO<sub>2</sub> surface layer onto Ti implants for improved biocompatibility. *Surf. Coat. Technol.* **2014**, *251*, 226–231.
- (15) Karthika, V.; Kaleeswarran, P.; Gopinath, K.; Arumugam, A.; Govindarajan, M.; Alharbi, N. S.; Khaled, J. M.; Al-Anbr, M. N.; Benelli, G. Biocompatible properties of nano-drug carriers using TiO<sub>2</sub>-Au embedded on multiwall carbon nanotubes for targeted drug delivery. *Mater. Sci. Eng., C* **2018**, *90*, 589–601.
- (16) Awad, N. K.; Edwards, S. L.; Morsi, Y. S. A review of TiO<sub>2</sub> NTs on Ti metal: Electrochemical synthesis, functionalization and potential use as bone implants. *Mater. Sci. Eng., C* **2017**, *76*, 1401–1412.
- (17) Yu, W.-q.; Jiang, X.-q.; Zhang, F.-q.; Xu, L. The effect of anatase TiO<sub>2</sub> nanotube layers on MC3T3-E1 preosteoblast adhesion, proliferation, and differentiation. *J. Biomed. Mater. Res., Part A* **2010**, *94*, 1012–1022.
- (18) Sun, X.; Xu, C.; Wu, G.; Ye, Q.; Wang, C. Poly(Lactic-co-Glycolic Acid): Applications and Future Prospects for Periodontal Tissue Regeneration. *Polymers* **2017**, *9*, 189.
- (19) Schliecker, G.; Schmidt, C.; Fuchs, S.; Wombacher, R.; Kissel, T. Hydrolytic degradation of poly(lactide-co-glycolide) films: effect of oligomers on degradation rate and crystallinity. *Int. J. Pharm.* **2003**, *266*, 39–49.
- (20) Witt, C.; Kissel, T. Morphological characterization of microspheres, films and implants prepared from poly(lactide-co-glycolide) and ABA triblock copolymers: is the erosion controlled by degradation, swelling or diffusion? *Eur. J. Pharm. Biopharm.* **2001**, *51*, 171–181.
- (21) Sun, Y.-S.; Lin, Y.-A.; Huang, H.-H. Using Genipin to Immobilize Bone Morphogenetic Protein-2 on Zirconia Surface for Enhancing Cell Adhesion and Mineralization in Dental Implant Applications. *Polymers* **2020**, *12*, 2639.
- (22) Campos, D. M.; Gritsch, K.; Salles, V.; Attik, G. N.; Grosgeat, B. Surface Entrapment of Fibronectin on Electrospun PLGA Scaffolds for Periodontal Tissue Engineering. *Biores. Open Access* **2014**, *3*, 117–126.
- (23) Wang, T.; Weng, Z.; Liu, X.; Yeung, K. W. K.; Pan, H.; Wu, S. Controlled release and biocompatibility of polymer/titania nanotube array system on titanium implants. *Bioact. Mater.* **2017**, *2*, 44–50.
- (24) Owen, G. R.; Jackson, J. K.; Chehroudi, B.; Brunette, D. M.; Burt, H. M. An in vitro study of plasticized poly(lactic-co-glycolic acid) films as possible guided tissue regeneration membranes: material properties and drug release kinetics. *J. Biomed. Mater. Res., Part A* **2010**, *95A*, 857–869.
- (25) Ma, A.; Shang, H.; Song, Y.; Chen, B.; You, Y.; Han, W.; Zhang, X.; Zhang, W.; Li, Y.; Li, C. Icarin-Functionalized Coating on TiO<sub>2</sub> Nanotubes Surface to Improve Osteoblast Activity In Vitro and Osteogenesis Ability In Vivo. *Coatings* **2019**, *9*, 327.
- (26) Fang, H.; Yang, X.; Chen, A.; Luo, Y. Effect of rhBMP-2 and osteogenic reagents on proliferation and differentiation of bone marrow stromal cells in rats. *J. Huazhong Univ. Sci. Technol., Med. Sci.* **2007**, *27*, 561–563.
- (27) Li, Y.; Song, Y.; Ma, A.; Li, C. Surface Immobilization of TiO<sub>2</sub> Nanotubes with Bone Morphogenetic Protein-2 Synergistically Enhances Initial Preosteoblast Adhesion and Osseointegration. *BioMed Res. Int.* **2019**, *2019*, 5697250.
- (28) Smith, L. J.; Swaim, J. S.; Yao, C.; Haberstroh, K. M.; Nauman, E. A.; Webster, T. J. Increased osteoblast cell density on nanostructured PLGA-coated nanostructured titanium for orthopedic applications. *Int. J. Nanomed.* **2007**, *2*, 493–499.
- (29) Escobar, A.; Muzzio, N.; Coy, E.; Liu, H.; Bindini, E.; Andreozzi, P.; Wang, G. C.; Angelome, P.; Delcea, M.; Grzelczak, M.; Moya, S. E. Antibacterial Mesoporous Titania Films with Embedded Gentamicin and Surface Modified with Bone Morphogenetic Protein 2 to Promote Osseointegration in Bone Implants. *Adv. Mater. Interfaces* **2019**, *6*, 1801648.
- (30) Um, S.; Kim, H. Y.; Lee, J.-H.; Song, I.-S.; Seo, B. M. TSG-6 secreted by mesenchymal stem cells suppresses immune reactions influenced by BMP-2 through p38 and MEK mitogen-activated protein kinase pathway. *Cell Tissue Res.* **2017**, *368*, 551–561.
- (31) Marinucci, L.; Balloni, S.; Becchetti, E.; Belcastro, S.; Guerra, M.; Calvitti, M.; Lilli, C.; Calvi, E. M.; Locci, P. Effect of titanium surface roughness on human osteoblast proliferation and gene expression in vitro. *Int. J. Oral Maxillofac. Implants* **2006**, *21*, 719–725.
- (32) Zhang, X.; Yu, Q.; Wang, Y.-a.; Zhao, J. Dose reduction of bone morphogenetic protein-2 for bone regeneration using a delivery system based on lyophilization with trehalose. *Int. J. Nanomed.* **2018**, *13*, 403–414.
- (33) Wang, F. F.; Li, Y.; Liu, H. C. A study on PLGA sustained release icaritin/titanium dioxide nanotube composite coating. *Eur. Rev. Med. Pharmacol. Sci.* **2019**, *23*, 911–917.

(34) Yang, D. H.; Lee, D.-W.; Kwon, Y.-D.; Kim, H. J.; Chun, H. J.; Jang, J. W.; Khang, G. Surface modification of titanium with hydroxyapatite-heparin-BMP-2 enhances the efficacy of bone formation and osseointegration *in vitro* and *in vivo*. *J. Tissue Eng. Regen. Med.* **2015**, *9*, 1067–1077.

(35) Maxfield, J. E.; Selfridge, R. G. The surface area of a screw. *Appl. Sci. Res., Sect. A* **1959**, *8*, 377–385.